THE JOURNAL OF PHYSICAL CHEMISTRY LETTERS
A JOURNAL OF THE AMERICAN CHEMICAL SOCIETY

pubs.acs.org/JPCL

Letter

An Efficient Reactive Force Field without Explicit Coordination Dependence for Studying Caustic Aluminum Chemistry

Maxime Pouvreau,* Qing Guo, Hsiu-Wen Wang, Gregory K. Schenter, Carolyn I. Pearce, Aurora E. Clark,* and Kevin M. Rosso*

Cite This: *J. Phys. Chem. Lett.* 2023, 14, 6743−6748

Read Online

ACCESS | Metrics & More | Article Recommendations | Supporting Information

ABSTRACT: Reactive force fields (RFFs) are an expedient approach to sample chemical reaction paths in complex systems, relative to density functional theory. However, there is continued need to improve efficiencies, specifically in systems that have slow transverse degrees of freedom, as in highly viscous and superconcentrated solutions. Here, we present an RFF that is differentiated from current models (e.g., ReaxFF) by omitting explicit dependence on the atom coordination and employing a small parameter set based on Lennard-Jones, Gaussian, and Stillinger−Weber potentials. The model was parametrized from AIMD simulation data and is used to model aluminate reactivity in sodium hydroxide solutions with extensive validation against experimental radial distribution functions, computed free energy profiles for oligomerization, and formation energies. The model enables simulation of early stage $Al(OH)_3$ nucleation which has significant relevance to industrial processing of aluminum *and* has a computational cost that is *reduced by 1 order of magnitude* relative to ReaxFF.

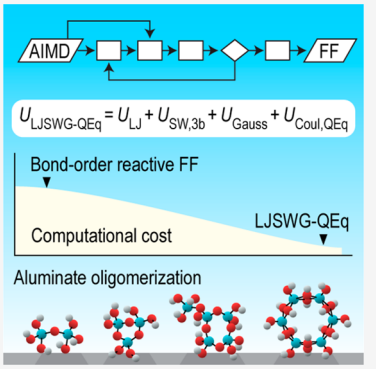

Reactive force fields are an important tool in classical simulations of systems in complex environments that induce bond breaking or forming reactions. ReaxFF,[1,2] COMB,[3,4] and the earlier Tersoff[5] and REBO[6]/AIREBO[7] are called bond order reactive potentials, where the bond order depends on atom coordination. The charge of an atom may also depend on its chemical environment as implemented in ReaxFF and COMB, which use the electronegativity equalization[8] (EEM) or charge equilibration (QEq)[9] methods. Bond order potentials exhibit up to 2 orders of magnitude higher computational cost compared to their nonreactive counterparts, and their parametrization is complex because of a large optimization space. For example, there are more than 100 tunable parameters for a 3-element ReaxFF set.[10] As an alternative, prior work has employed fixed-charge, nonbonded two-body- and three-body-based dissociative force fields[11−14] to reproduce realistic lifetimes of species and proton transfer rates and, at the same time, reduce the computational effort by 1 order of magnitude compared to ReaxFF.[14,11] Nonbonded terms without coordination dependence have already been augmented with charge equilibration to describe the energetics of minerals,[15] but not to model reactions yet.

This work continues prior development by employing existing potentials (Lennard-Jones, Stillinger−Weber, Gaussian terms) and variable charges based on QEq (referred to hereafter as the LJSWG-QEq model). Using LAMMPS[16] version 22 Dec 2022, this approach results in a 10-fold improvement in efficiency with respect to ReaxFF (2017 water set[17]) as tested for a simulation box of 5000 water molecules using one 64 core single socket AMD Rome node. It further is only a 4-fold increase in computational time relative to a SPC water model.[18] The increased computational efficiency allows reactive events with a relatively low activation energy to be sampled more effectively without the need for biasing, and in the case of systems that have slow transverse degrees of freedom (e.g., high viscosity), enhanced sampling methods along a reaction coordinate are much more expedient. We demonstrate the parametrization for solutions containing aluminate and/or sodium hydroxide across a range of concentrations where there is significant interconversion between aluminate species and other reactions. Indeed, the force field will be first applied to understand early stage nucleation of $Al(OH)_3$ and other solid phases.

To maintain simplicity without compromising accuracy, the functional form was kept minimal by excluding unnecessary bonding terms and more complex forms that only yielded marginal improvement—explanations can be found in the Supporting Information. The LJSWG-QEq model combines the following potentials:

(i) Lennard-Jones terms for the O−O, Al−O, O−H, and Na−O pairs:

Received: May 3, 2023
Accepted: July 7, 2023
Published: July 20, 2023

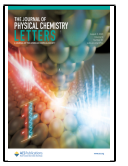

https://doi.org/10.1021/acs.jpclett.3c01176
J. Phys. Chem. Lett. 2023, 14, 6743−6748

$$U_{LJ}(r_{ij}) = 4\varepsilon_{ij}\left[\left(\frac{\sigma_{ij}}{r_{ij}}\right)^{12} - \left(\frac{\sigma_{ij}}{r_{ij}}\right)^{6}\right] \quad (1)$$

Note that a linear term is subtracted from the potential to ensure it goes continuously to zero at the cutoff.[19]

(ii) Gaussian terms[20] for the Al−O, O−H, and Al−Al pairs:

$$U_{gauss}(r_{ij}) = \frac{H_{ij}}{\sigma_{h,ij}\sqrt{2\pi}}\exp\left(-\frac{(r_{ij} - r_{mh,ij})^2}{2\sigma_{h,ij}^2}\right) \quad (2)$$

(iii) Nonbonded angle terms from the Stillinger−Weber potential[21] for the H−O−H and Al−O−H angles:

$$\phi_3(r_{ij}, r_{ik}, \theta_{ijk}) = \lambda_{ijk}\varepsilon_{ijk}[\cos\theta_{ijk} - \cos\theta_{0ijk}]^2\exp\left(\frac{\gamma_{ij}\sigma_{ij}}{r_{ij} - a_{ij}\sigma_{ij}}\right)\exp\left(\frac{\gamma_{ik}\sigma_{ik}}{r_{ik} - a_{ik}\sigma_{ik}}\right) \quad (3)$$

where ε_{ijk}, a_{ij}, and a_{ik} were all fixed to 1 due to the fact the two-body terms of the Stillinger−Weber potential are not used here.

(iv) An electrostatic potential with variable charges that are obtained self-consistently by EEM/QEq:[8,9,22]

$$E(q_1, q_2, ..., q_N) = \sum_{i=1}^{N}\left(\chi_i^0 q_i + \frac{1}{2}J_{ii}^0 q_i^2 + \sum_{j>1}^{N} J_{ij}q_i q_j\right) \quad (4)$$

where N is the total number of atoms in the system, $E_i(0)$ is the charge reference point at $q = 0$, χ_i^0 is the electronegativity, q_i and q_j are the charges, and J_{ii} is the atomic hardness. QEq only differs from EEM by the form of J_{ij} and because it uses an iterative procedure for hydrogen charges contrary to EEM. Here the pairwise J_{ij} term is different from that in the original EEM and QEq publications and uses a shielded coulomb potential first employed in ReaxFF[1] of the form

$$J_{ij} = \frac{1}{[r_{ij}^3 + (1/\gamma_{ij})^3]^{1/3}} \quad (5)$$

The variable charge method will be termed QEq for brevity. The Coulombic interactions in periodic systems were computed using a long-range solver.[23]

The fitting procedure is summarized in Figure 1. Fitting was based on minimization of the objective function:

$$f = \frac{W_E\mathrm{Err}(E) + W_{F_A}\mathrm{Err}(F_A) + W_{F_B}\mathrm{Err}(F_B) + W_q\mathrm{Err}(q) + W_p\mathrm{Err}(P)}{W_E + W_{F_A} + W_{F_B} + W_q + W_P} \quad (6)$$

with Err(x) the errors, E the energies, $\boldsymbol{F}_A$ and $\boldsymbol{F}_B$ two types of forces defined below, q the point charges, and $\mathbf{p}$ the pressure tensor all obtained using LAMMPS single-point calculations on the reference structures. The expressions of the individual error terms are given in the Supporting Information. The weights of the terms were selected to equal their level of magnitude.

The training set comprises 37 subsets spanning 598 atomic configurations and is detailed in Table S1 (with details concerning the AIMD and static density functional theory (DFT) calculations). The training data encompass $NaOH_{(aq)}$ solutions, aluminate species ($Al(OH)_4^-$ monomers, dimers, trimers, and hexamers) in $NaOH_{(aq)}$, other water and ion−water gas-phase clusters, and solid-state structures. The goal is to develop a force field that yields the correct structures and aluminate interconversion energies in $NaOH_{(aq)}$. Multiple methods were employed during force field parameterization,

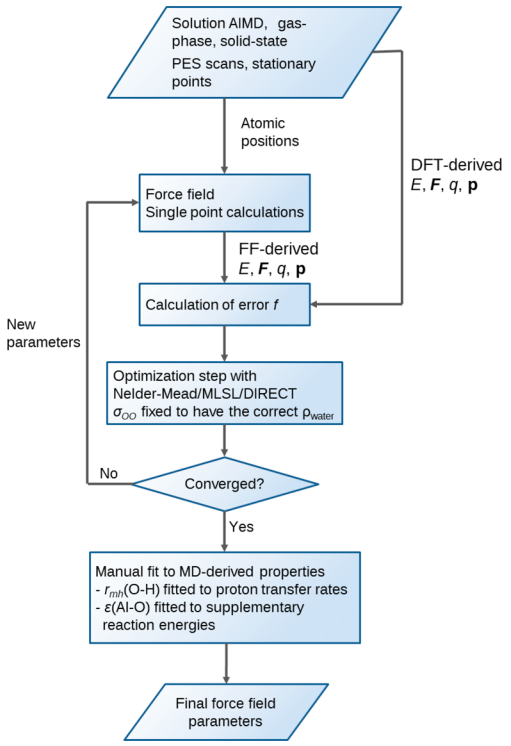

Figure 1. Force field fitting workflow.

including unbiased and biased AIMD trajectories, potential energy surface (PES) scans (simple scans, nudged elastic band, intrinsic reaction coordinate), or geometry optimization when only the reactant and product states are included. In eq 6, $\boldsymbol{F}_A$ corresponds to forces of the geometry-optimized structures, which by definition should be zero, and $\boldsymbol{F}_B$ corresponds to all the other forces. In the gas-phase subset, electrostatic potential-derived point charges were also computed and included. The methodology employed for biasing AIMD is detailed in the Supporting Information. Importantly, the current parametrization scheme is different from past molecular physics-based RFF parametrization schemes in that the effect of the solution on reactivity is already part of the training set, which to our knowledge has never been done.

The minimization of f was based on a local minimization using an adaptive Nelder−Mead from the SciPy package version 1.7.0,[24] and global minimization (MLSL_LDS,[25] DIRECT_L_RAND[26] algorithms) was performed using NLopt python package.[27] Once an approximate set of parameters $\{x_i\}$ was found using the local algorithm, the parameters were globally optimized using the boundaries $[x_i - \alpha x_i; x_i + \alpha x_i]$ with $0 < \alpha < 1$. Three parameters were tuned manually to ensure certain properties were correctly reproduced:

- σ(O−O) to obtain the experimental water density at 300 K; the optimal value was then fixed in the automated fit.
- The Gaussian parameter r_{mh}(O−H) was tuned to reproduce proton transfer rates in NaOH(aq) (see the Supporting Information).
- The Lennard-Jones well depth ε(Al−O) to improve oligomerization energetics; the results of the FF with the original and modified values are described in the following.

https://doi.org/10.1021/acs.jpclett.3c01176
J. Phys. Chem. Lett. 2023, 14, 6743−6748

The two last adjustments only resulted in a 5% increase of the value of f while greatly improving the two target properties. The final parameters are listed in Table 1.

Table 1. LJSWG-QEq Parameters[a]

QEq	χ (kcal/mol)	η (kcal/mol)	γ (Å)
Al	23.8613	332.6560	0.00987
O	680.2788	329.3557	0.11367
H	209.1501	597.8199	0.27432
Na	21.6300	535.0652	2.24750
Lennard-Jones		ε (kcal/mol)	σ (Å)
Al−O		1.740000	1.8601
O−O		0.048769	3.2500
O−H		0.064643	1.2550
Na−O		0.004130	3.4416
Gaussian	H(Å·kcal/mol)	r_{mh} (Å)	σ_h (Å)
Al−Al	1.0020	2.8207	0.2075
Al−O	−0.7230	1.5926	0.0550
O−H	−0.4747	1.0700	0.0759
Stillinger−Weber angle term ijk	λ_{ijk} (kcal/mol)	σ_{ij} (Å)	γ_{ij}	$\cos(\theta_{0ijk})$
H−O−H	1902.94	2.33489[b]	1.09844	−0.161679
Al−O−H	1437.62	5.08380[b]	1.70690	−0.309313

[a]The force field parameters are given in LAMMPS format in the Supporting Information. [b]Also act as cutoffs for the force-shifted Lennard-Jones potentials (energies and forces are continuous; see text).

Using the final fitted values, we first compare the results from LJSWG-QEq classical molecular dynamics with experiment, AIMD, and other force fields for the radial distribution functions (RDFs) of water−water and ion−water pairs at infinite dilution and the total neutron and X-ray RDFs for a sodium deuteroxide and an aluminate solution (Figures 2 and S3). The full description of the results is provided in the Supporting Information, and the most important findings are presented here. The predicted water−water RDF is close to that of dedicated water models, where $g_{OO}(r)$ is provided in Figure 2a and $g_{OH}(r)$ and $g_{HH}(r)$ together with the running coordination numbers are given in Figure S1. The positions of the first O−O peak and CN(O−O) are both close to experiment and water models, and the height is overestimated like all water models based on Lennard-Jones. The overestimation of hydroxide hydration by nonpolarizable models is corrected by LJSWG-QEq with CN(O_{OH}^-−O_w) within 13% of AIMD (w: water), whereas it is 30% for nonpolarizable models (Figure S2). Simulations were also conducted for highly concentrated sodium deuteroxide (18.056 m NaOD) solutions and a solution of $Al(OD)_4^-$ in NaOD(aq) (0.500 m Al, 2.703 m NaOD). The LJSWG-QEq X-ray and neutron radial RDFs for NaOD(aq) are presented in Figure 2c,d[28] and the RDF of the aluminate solution (Figure S3) follows the same trends as that of the NaOD(aq). For neutron RDFs, all models overestimate the RDF intensity in the 1.6−2.4 Å region, originating from hydrogen bonding and first-shell Na−O peaks (due to the hard Lennard-Jones repulsion in r^{-12}), and underestimate the intensity of a broad feature at 3.2 Å, associated with second-shell contributions of O_{OD}^-−D_w. The LJSWG-QEq model introduces two improvements in the neutron RDF at 2.4 and 2.7 Å, eliminating the sharp feature observed for the Drude model and decreasing the height of the O_{OD}^-−O_w peak. The simulated LJSWG-QEq X-ray RDF underestimates the height of the Na−O peak with respect to experiment and the Drude model, but the agreement with experiment is superior to the Drude and the nonpolarizable models for the O_{OD}^-−O_w peak.

The energies of formation (ΔE) for a variety of aluminate oligomers, including different types of Al−Al bridging (oxo-, hydroxo-) and coordination states (4, 5, 6), are shown in Table 2 together with differences weighted by the inverse of the number of Al (the error being size-dependent) for several methods. Reference energies were calculated using the DLPNO-CCSD(T)/def2-TZVPPD (SMD, water)//M062X-

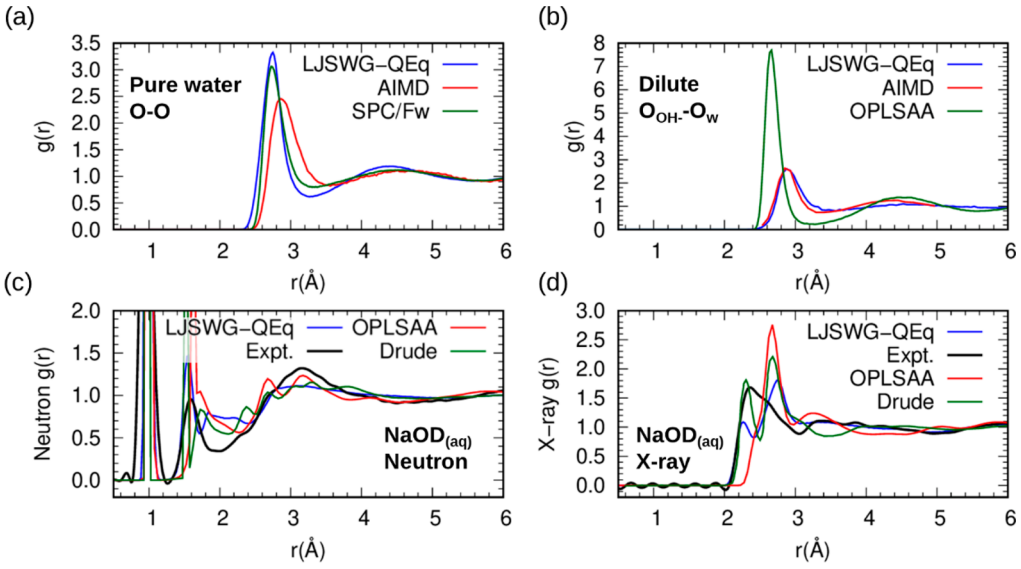

Figure 2. LJSWG-QEq radial distribution functions for (a) the O−O pair of liquid water (w) with a comparison with AIMD and SPC/Fw, (b) the O_{OH}^-−O_w pair with a comparison to AIMD[29] and a nonpolarizable classical MD (OPLSAA + SPC/Fw). (c) Neutron and (d) X-ray radial distribution functions of a highly concentrated NaOD solution (18.056 m) with a comparison to experimental and nonpolarizable models (OPLSAA + SPC/E) and polarizable Drude model from Semrouni et al.[28]

https://doi.org/10.1021/acs.jpclett.3c01176
J. Phys. Chem. Lett. 2023, 14, 6743−6748

Table 2. Errors of Aluminate Oligomerization Reaction Energies in Water Weighted by the Number of Al for Different Methods (kcal/mol)[a]

	$(\Delta E - \Delta E_{ref.})/N(\mathrm{Al})$			
			LJSWG-QEq	
	DFT	PM6	orig.	mod.
$2\ Al(OH)_4^- \rightleftharpoons Al_2O(OH)_6^{2-} + H_2O$	−0.45	2.80	4.83	1.24
$2\ Al(OH)_4^- \rightleftharpoons Al_2(OH)_7^- + OH^-$	0.01	−1.90	−14.43	−7.76
$2\ Al(OH)_4^- \rightleftharpoons Al_2O_2(OH)_4^{2-} + 2\ H_2O$	0.37	−1.04	−7.81	−9.69
$2\ Al(OH)_4^- + 2\ OH^- \rightleftharpoons Al_2(OH)_{10}^{4-}$	−4.32	15.46	−1.28	4.93
$3\ Al(OH)_4^- \rightleftharpoons Al_3O_3(OH)_6^{3-} + 3\ H_2O$	−0.21	4.51	−1.84	−1.63
$3\ Al(OH)_4^- \rightleftharpoons Al_3O_2(OH)_8^{3-} + 2\ H_2O$	−0.49	4.49	−1.82	−0.78
$3\ Al(OH)_4^- + OH^- \rightleftharpoons Al_3O_4(OH)_5^{4-} + 4\ H_2O$	−0.50	4.11	−6.12	−7.36
$3\ Al(OH)_4^- \rightleftharpoons Al_3(OH)_{12}^{3-}$	−2.31	8.83	5.99	1.97
$4\ Al(OH)_4^- \rightleftharpoons Al_4O_4(OH)_8^{4-} + 4\ H_2O$	−0.87	6.05	2.91	−0.21
$4\ Al(OH)_4^- \rightleftharpoons Al_4(OH)_{16}^{4-}$	−2.65	9.48	8.42	2.63
Mean absolute error	**1.22**	**5.87**	**5.55**	**3.82**

[a]Reference (ref.) energies: DLPNO-CCSD(T)/def2-TZVPPD (SMD, water)//DFT (SMD, water). DFT: M062X-D3/def2-TZVPPD. orig.: original, ε(Al−O) = 0.388 kcal/mol; mod.: modified, ε(Al−O)=1.740 kcal/mol. The oligomer geometries are provided in Figure S4.

D3/def2-TZVPPD(SMD, water)[31−33] level of theory. The LJSWG-QEq reaction energies were averaged from MD simulations with fixed solutes (details in the Supporting Information). The well depth of the Al−O Lennard-Jones term potential ε(Al−O) was fine-tuned manually following the automated fit to improve the mean absolute error (MAE) of the reaction energies with respect to the reference values. The MAE of the original form of the force field using ε(Al−O) = 0.388 kcal/mol (5.55 kcal/mol) is already smaller than that of PM6,[34] a general-purpose semiempirical method (5.87 kcal/mol). Increasing ε(Al−O) from 0.388 to 1.740 kcal/mol brings the MAE down to 3.82 kcal/mol to compare with the DFT (M062X-D3/TZVPPD) value of 1.22 kcal/mol. In particular, it tends to strongly reduce the change in energy of the formation of oligomers associated with an increase in CN(Al−O) with respect to the monomer, such as $Al_3(OH)_{12}^{3-}$ or $Al_4(OH)_{16}^{4-}$ (consisting of 5- and 6-coordinated Al).

Next in the LJSWG-QEq validation, we examine the reactivity of aluminate through potential of mean force (PMF) simulations and energies of formation for a variety of aluminate oligomers. The PMF for the formation of the dihydroxo-bridged dimer, $Al_2(OH)_8^{2-}$, is shown in Figure 3. The dimer is formed by two successive bridges and is very similar to the PMF derived from self-consistent-charge density-functional tight-binding (SCC-DFTB) MD,[30] with a difference of only 2 kcal/mol. The reaction intermediate and the product are stabilized by ∼4 and ∼8 kcal/mol due to the increase of the parameter ε(Al−O), which is consistent with the formation of oligomers accompanied by an increase in CN(Al−O).

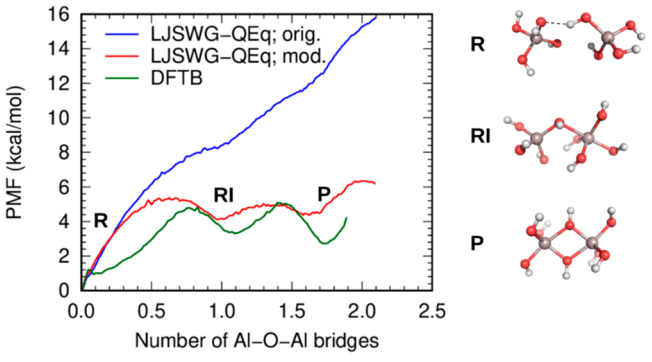

Figure 3. Potential of mean force of the formation of the aluminate dihydroxo-bridged dimer $Al_2(OH)_8^{2-}$ and comparison with SCC-DFTB.[30] The original (orig.) and modified (mod.) versions correspond to ε(Al−O) = 0.388 kcal/mol and ε(Al−O) = 1.740 kcal/mol, respectively.

The successful performance of the LJSWG-QEq model in studying aluminate reactivity shows that the functional form has the correct physics for this problem. Recall that reactive bond order potentials originate from the idea that an increase of the AB_n atom coordination number should be accompanied by a decrease in the individual AB bond strengths.[5] The value of the MAE in Table 2, small for an empirical method, shows that semiquantitative modeling of aluminate oligomeric reactions is possible even with a diverse population of coordination numbers. This is an indication that, for Al solution chemistry, there is an overlap between the effect of coordination number dependence and of QEq on the relationship between coordination number and bond strength—consistent with the dative (or coordinate covalent) nature of Al−O bonds—and that bond order terms dependent on coordination can be omitted in order to save the associated computational cost. Based on the validation presented here, this idea could be extended to other systems. However, for some chemical systems and properties, situations likely exist where charge equilibration is not sufficient and where coordination-dependent bond orders need to be applied to achieve satisfactory accuracy; empirical testing will be needed to determine if this is true.

In summary, a new and efficient reactive force field (LJSWG-QEq) was developed for oligomerization in sodium aluminate solutions. LJSWG-QEq omits bond-order-based terms based on atom coordination and uses existing potentials and variable charges based on QEq charge equilibration, resulting in only 37 parameters for 4 elements and high efficiency. The parametrization process is based on the minimization of the error with respect to energies, forces, point charges, and pressure tensors collected from ab initio molecular dynamics of aqueous solutions and static DFT. Therefore, the training set includes the effect of the solution on aluminate reactivity which, as far as we know, has never been accomplished. MD using LJSWG-QEq was used to obtain RDFs for water−water,

https://doi.org/10.1021/acs.jpclett.3c01176
J. Phys. Chem. Lett. 2023, 14, 6743−6748

ion−water pairs, and sodium deuteroxide and aluminate solutions. Overall, the magnitude of the differences is similar to other force fields with an improvement in some aspects, e.g., the coordination of hydroxide by water molecules. The errors of the energies of formation for different types of aluminate oligomers relative to DLPNO-CCSD(T) including various Al−Al bridging and coordination states were computed and compared to reference values for several methods. Fine-tuning ε(Al−O) reduces the MAE of the original force field to a value intermediate between that of a semiempirical method and that of the M062X-D3 DFT functional. Additionally, the free energy profile of the formation of the dihydroxo-bridged dimer $Al_2(OH)_8^{2-}$ from two $Al(OH)_4^-$ is shown to be similar to the PMF derived from SCC-DFTB MD from previous work. This work shows that within a given set of reactions, omitting coordination-dependent terms and keeping only a subset of the two- or three-body terms can result in satisfactory accuracy while decreasing the computational cost by about 1 order of magnitude.

■ ASSOCIATED CONTENT

Supporting Information

The Supporting Information is available free of charge at https://pubs.acs.org/doi/10.1021/acs.jpclett.3c01176.

Force field parameters in LAMMPS format (ZIP)

Parameterization: tests of different functional forms, formulas of the terms of the objective function, tuning of the Gaussian parameter r_{mh}(O−H), full training set (Table S1), computational methods for AIMD and static DFT; methods used in the validation of the force field: solution preparation and experimental RDFs, MD simulations, computational RDFs, potential of mean force, calculation of oligomerization energies; supplementary RDFs: water−water (pure water, Figure S1), Na^+−water (dilute solution, Figure S2), and NaOD(aq) and sodium aluminate solutions (Figure S3); Oligomer geometries (Figure S4) (PDF)

Transparent Peer Review report available (PDF)

■ AUTHOR INFORMATION

Corresponding Authors

Maxime Pouvreau − *Pacific Northwest National Laboratory, Richland, Washington 99352, United States;* orcid.org/0000-0002-9015-5086; Email: mx.pouvreau@gmail.com

Aurora E. Clark − *Department of Chemistry, University of Utah, Salt Lake City, Utah 84112, United States;* orcid.org/0000-0001-9381-721X; Email: aurora.clark@utah.edu

Kevin M. Rosso − *Pacific Northwest National Laboratory, Richland, Washington 99352, United States;* orcid.org/0000-0002-8474-7720; Email: kevin.rosso@pnnl.gov

Authors

Qing Guo − *Department of Chemistry, University of Utah, Salt Lake City, Utah 84112, United States*

Hsiu-Wen Wang − *Chemical Sciences Division, Oak Ridge National Laboratory, Oak Ridge, Tennessee 37831, United States;* orcid.org/0000-0002-2802-4122

Gregory K. Schenter − *Pacific Northwest National Laboratory, Richland, Washington 99352, United States*

Carolyn I. Pearce − *Pacific Northwest National Laboratory, Richland, Washington 99352, United States;* orcid.org/0000-0003-3098-1615

Complete contact information is available at: https://pubs.acs.org/10.1021/acs.jpclett.3c01176

Notes

The authors declare no competing financial interest.

■ ACKNOWLEDGMENTS

The research was supported by IDREAM (Interfacial Dynamics in Radioactive Environments and Materials), an Energy Frontier Research Center funded by the U.S. Department of Energy (DOE), Office of Science, Basic Energy Sciences (BES) (FWP 68932). Molecular simulations utilized resources from PNNL Research Computing, the Center for Institutional Research Computing at Washington State University, and the Center for High Performance Computing at the University of Utah. The research at the NOMAD instrument, Spallation Neutron Source at Oak Ridge National Laboratory, was supported by the Scientific User Facilitates Division, BES, DOE. The research at the 11-ID-B beamline, Advanced Photon Source, Argonne National Laboratory was also supported by the Scientific User Facilitates Division, BES, DOE. PNNL is a multiprogram national laboratory operated for DOE by Battelle Memorial Institute operating under Contract No. DE AC05-76RL0-1830.

■ REFERENCES

(1) van Duin, A. C. T.; Dasgupta, S.; Lorant, F.; Goddard, W. A. ReaxFF: A Reactive Force Field for Hydrocarbons. *J. Phys. Chem. A* **2001**, *105* (41), 9396−9409.

(2) Chenoweth, K.; van Duin, A. C. T.; Goddard, W. A. ReaxFF Reactive Force Field for Molecular Dynamics Simulations of Hydrocarbon Oxidation. *J. Phys. Chem. A* **2008**, *112* (5), 1040−1053.

(3) Shan, T.-R.; Devine, B. D.; Kemper, T. W.; Sinnott, S. B.; Phillpot, S. R. Charge-Optimized Many-Body Potential for the Hafnium/Hafnium Oxide System. *Phys. Rev. B* **2010**, *81* (12), 125328.

(4) Liang, T.; Shan, T.-R.; Cheng, Y.-T.; Devine, B. D.; Noordhoek, M.; Li, Y.; Lu, Z.; Phillpot, S. R.; Sinnott, S. B. Classical Atomistic Simulations of Surfaces and Heterogeneous Interfaces with the Charge-Optimized Many Body (COMB) Potentials. *Mater. Sci. Eng. R Rep.* **2013**, *74* (9), 255−279.

(5) Tersoff, J. New Empirical Approach for the Structure and Energy of Covalent Systems. *Phys. Rev. B* **1988**, *37* (12), 6991−7000.

(6) Brenner, D. W. Empirical Potential for Hydrocarbons for Use in Simulating the Chemical Vapor Deposition of Diamond Films. *Phys. Rev. B* **1990**, *42* (15), 9458−9471.

(7) Brenner, D. W.; Shenderova, O. A.; Harrison, J. A.; Stuart, S. J.; Ni, B.; Sinnott, S. B. A Second-Generation Reactive Empirical Bond Order (REBO) Potential Energy Expression for Hydrocarbons. *J. Phys.: Condens. Matter* **2002**, *14* (4), 783.

(8) Mortier, W. J.; Ghosh, S. K.; Shankar, S. Electronegativity-Equalization Method for the Calculation of Atomic Charges in Molecules. *J. Am. Chem. Soc.* **1986**, *108* (15), 4315−4320.

(9) Rappe, A. K.; Goddard, W. A. Charge Equilibration for Molecular Dynamics Simulations. *J. Phys. Chem.* **1991**, *95* (8), 3358−3363.

(10) Nayir, N.; van Duin, A. C. T.; Erkoc, S. Development of the ReaxFF Reactive Force Field for Inherent Point Defects in the Si/Silica System. *J. Phys. Chem. A* **2019**, *123* (19), 4303−4313.

(11) Wiedemair, M. J.; Hofer, T. S. Towards a Dissociative SPC-like Water Model − Probing the Impact of Intramolecular Coulombic Contributions. *Phys. Chem. Chem. Phys.* **2017**, *19* (47), 31910−31920.

(12) Hofer, T. S.; Wiedemair, M. J. Towards a Dissociative SPC-like Water Model II. The Impact of Lennard-Jones and Buckingham Non-Coulombic Forces. *Phys. Chem. Chem. Phys.* **2018**, *20* (45), 28523−28534.
(13) Mahadevan, T. S.; Garofalini, S. H. Dissociative Water Potential for Molecular Dynamics Simulations. *J. Phys. Chem. B* **2007**, *111* (30), 8919−8927.
(14) Mahadevan, T. S.; Garofalini, S. H. Dissociative Chemisorption of Water onto Silica Surfaces and Formation of Hydronium Ions. *J. Phys. Chem. C* **2008**, *112* (5), 1507−1515.
(15) Sefcik, J.; Demiralp, E.; Cagin, T.; Goddard, W. A. Dynamic Charge Equilibration-Morse Stretch Force Field: Application to Energetics of Pure Silica Zeolites. *J. Comput. Chem.* **2002**, *23* (16), 1507−1514.
(16) Plimpton, S. Fast Parallel Algorithms for Short-Range Molecular Dynamics. *J. Comput. Phys.* **1995**, *117* (1), 1−19.
(17) Zhang, W.; van Duin, A. C. T. Second-Generation ReaxFF Water Force Field: Improvements in the Description of Water Density and OH-Anion Diffusion. *J. Phys. Chem. B* **2017**, *121* (24), 6021−6032.
(18) Wu, Y. J.; Tepper, H. L.; Voth, G. A. Flexible Simple Point-Charge Water Model with Improved Liquid-State Properties. *J. Chem. Phys.* **2006**, *124* (2), 024503.
(19) Toxvaerd, S.; Dyre, J. C. Communication: Shifted Forces in Molecular Dynamics. *J. Chem. Phys.* **2011**, *134* (8), 081102.
(20) Lenart, P. J.; Jusufi, A.; Panagiotopoulos, A. Z. Effective Potentials for 1:1 Electrolyte Solutions Incorporating Dielectric Saturation and Repulsive Hydration. *J. Chem. Phys.* **2007**, *126* (4), 044509.
(21) Stillinger, F. H.; Weber, T. A. Computer Simulation of Local Order in Condensed Phases of Silicon. *Phys. Rev. B* **1985**, *31* (8), 5262−5271.
(22) Nakano, A. Parallel Multilevel Preconditioned Conjugate-Gradient Approach to Variable-Charge Molecular Dynamics. *Comput. Phys. Commun.* **1997**, *104* (1), 59−69.
(23) Hockney, R. W.; Eastwood, J. W. *Computer Simulation Using Particles*; 1988.
(24) Virtanen, P.; Gommers, R.; Oliphant, T. E.; Haberland, M.; Reddy, T.; Cournapeau, D.; Burovski, E.; Peterson, P.; Weckesser, W.; Bright, J.; et al. SciPy 1.0: Fundamental Algorithms for Scientific Computing in Python. *Nat. Methods* **2020**, *17* (3), 261−272.
(25) Rinnooy Kan, A. H. G.; Timmer, G. T. Stochastic Global Optimization Methods Part I: Clustering Methods. *Math. Program.* **1987**, *39* (1), 27−56.
(26) Gablonsky, J. M.; Kelley, C. T. *A Locally-Biased Form of the DIRECT Algorithm*.
(27) Johnson, S. G.; Schueller, J. *NLopt: Nonlinear Optimization Library*; Astrophys. Source Code Libr., 2021; ascl:2111.004.
(28) Semrouni, D.; Wang, H.-W.; Clark, S. B.; Pearce, C. L.; Page, K.; Schenter, G.; Wesolowski, D. J.; Stack, A. G.; Clark, A. E. Resolving Local Configurational Contributions to X-Ray and Neutron Radial Distribution Functions within Solutions of Concentrated Electrolytes − a Case Study of Concentrated NaOH. *Phys. Chem. Chem. Phys.* **2019**, *21* (13), 6828−6838.
(29) Bucher, D.; Gray-Weale, A.; Kuyucak, S. Ab Initio Study of Water Polarization in the Hydration Shell of Aqueous Hydroxide: Comparison between Polarizable and Nonpolarizable Water Models. *J. Chem. Theory Comput.* **2010**, *6* (9), 2888−2895.
(30) Pouvreau, M.; Martinez-Baez, E.; Dembowski, M.; Pearce, C. I.; Schenter, G. K.; Rosso, K. M.; Clark, A. E. Mechanisms of Al3+ Dimerization in Alkaline Solutions. *Inorg. Chem.* **2020**, *59* (24), 18181−18189.
(31) Riplinger, C.; Neese, F. An Efficient and near Linear Scaling Pair Natural Orbital Based Local Coupled Cluster Method. *J. Chem. Phys.* **2013**, *138* (3), 034106.
(32) Zhao, Y.; Truhlar, D. G. The M06 Suite of Density Functionals for Main Group Thermochemistry, Thermochemical Kinetics, Noncovalent Interactions, Excited States, and Transition Elements: Two New Functionals and Systematic Testing of Four M06-Class Functionals and 12 Other Functionals. *Theor. Chem. Acc.* **2008**, *120* (1−3), 215−241.
(33) Grimme, S.; Antony, J.; Ehrlich, S.; Krieg, H. A Consistent and Accurate Ab Initio Parametrization of Density Functional Dispersion Correction (DFT-D) for the 94 Elements H-Pu. *J. Chem. Phys.* **2010**, *132* (15), 154104.
(34) Stewart, J. J. P. Optimization of Parameters for Semiempirical Methods V: Modification of NDDO Approximations and Application to 70 Elements. *J. Mol. Model.* **2007**, *13* (12), 1173−1213.

https://doi.org/10.1021/acs.jpclett.3c01176
J. Phys. Chem. Lett. 2023, 14, 6743−6748